I J C T A, 9(1), 2016, pp. 45-60

Design of a Mowing Robot and Implementation of Its Dead Reckoning System

Chen Yang and Chung-Liang Chang*

Abstract: This study presents a prototype design of electric mowing robot. Its core system consists of a micro-controller, sensing modules (including ultrasonic sensors, laser range finder, electronic compass, and odometer), and power module, which allows the robot the ability to travel independently and complete obstacle avoidance. The data fed back by the electronic compass and odometer module can help obtain the heading of robot. Through dead reckoning, the dual motors can be driven in real time to adjust speed and position, and the information sent back by the laser ranging finder can provide information to the robot to determine areas that have not been mowed. The ultrasonic sensors are to perform obstacle avoidance capabilities. The dual front-motors of robot are driven by direct-current (DC) pulse width modulation (PWM) modules, while the mowing device trimmer head, installed at the bottom of the robot, uses jagged blade and a mowing plate. At the side of the mowing plate, a baffle is installed to avoid weeds and small stones. The heading control system can be implemented through a graphical user interface (GUI) for remote operation to perform manual and automatic mowing. The experimental results suggest that, in modified mowing paths, the ranging error of the mowing robot designed in this study is 3.2±0.1 (standard deviation [SD]) cm, and its maximum mowing coverage rate is about 90 %.

Additional index words.: Dead reckoning, micro-controller, graphical user interface

BACKGROUND

As technology continues to progress, intelligent robot technology has matured and been gradually introduced into public livelihood and military purposes. The autonomous robots include, cleaning robots [**1**], mining robots [**2**], gardening robots [**3**][**4**], mowing robots [**5**][**6**], and a variety of mobile-type robots [**7–9**] have been commercialized and marketed. Regarding the development of the mowing robots, from the early period conventional cylinder lawnmower to the modern human-pushed lawn mower, riding mowers, and knapsack mowers [**10**], the designs of the machines and systems are becoming increasingly lightweight and autonomous. In 2006, Nourani-Vatani proposed the large-scale autonomous mower [**11**], which integrated global positioning system (GPS) receiver, inertial measurement unit (IMU), laser scanner, and video camera for synchronous mapping in order to realize the purpose of random routing planning and virtual ground obstacle avoidance. In addition, some designs attempt to use sensor fusion method for positioning, and integrate GPS with vision, ultrasonic, or optical microelectromechanical sensors (MEMs) to complete automatic mowing [**12–14**]; however, as these mowers have very high development costs. In recent years, there are intelligent electric mowers available on the market [**15–18**], which are more suitable for mowing in a small area and are relatively inexpensive, and thus, are relatively easy to be accepted by the public. Therefore, under the premise of low-cost development, and in the case of a known mowing path, this study proposes using only the electronic compass and odometer to implement robot dead reckoning. Combined with a proportion-integral-derivative (PID) controller to precisely adjust the motor speed, it allows the robot to achieve short-distance straight traveling and cornering functions with high positioning accuracy.

* Department of Biomechatronics Engineering, National Pingtung University of Science and Technology, 91201, No. 1, Shuefu Road, Neipu, Pingtung County, Taiwan, R.O.C., *E-mail: chungliang@mail.npust.edu.tw*

In addition, the robot is installed with 6 sets of ultrasonic and laser modules, as well as the human-machine interface for remote operation, which empowers the mowing robot to have the capabilities of obstacle avoidance and orientation judgment of the area without mowing.

The remainder of this paper is organized as follows: Section 2 introduces the robot motion model, dead reckoning method, and rotation speed and rotation angle control principles; Section 3 describes the robot system design process, including the mechanical design, software design, and hardware architecture; Section 4 discusses the experimental results; Section 5 offers conclusions and suggestions for future works.

MATERIAL AND METHODS

This section describes the skid-steering wheeled robot's motion equations; dead reckoning; how to apply the PID method to achieve the purpose of controlling the rotation speed of both wheels; illustrates the robot's motion equations; elaborates on how to use the heading and rotation speed data obtained by the electric compass and odometer to complete the dead reckoning function, and describes the process of using the PID controller to control the left and right rotation speed of motor and rotation angle.

1. Robot mathematical model

It is presumed that the mobile robot's working environment is known, and the coordinate system of the robot is the same as that of the working space. Regarding the double-wheel robot motion model, if friction and attitude of the robot is not considered, the ideal motion equations are as shown in (1) and (2)

$$\dot{x} = \cos\theta \cdot v \tag{1}$$

$$\dot{y} = \sin\theta \cdot v \tag{2}$$

where $v = (V_R + V_L)/2$ denotes the linear speed of robot; $\dot{x}$ and $\dot{y}$ denotes the velocity of robot in the direct of the X-axis and Y-axis, respectively; and V_R and V_L denotes the speeds of the right wheel and left wheel, respectively. According to (3) and (4):

$$V_R = v + \frac{m\omega}{2} \tag{3}$$

$$V_L = v - \frac{m\omega}{2} \tag{4}$$

where *m* denotes the distance between the two wheels of the robot, and $\omega = \dot{\theta}$ represents the angular speed of robot. According to (1) to (4), the robot's linear speed and steering speed do not affect each other. Therefore, the user may adjust the rotation speed of both wheels to obtain the required linear speed and steering speed.

2. DEAD RECKONING

Dead reckoning is defined as the estimation of the next position by robot displacement $\Delta d_t = {(\Delta s_L + \Delta s_R)}/{2}$ and the direction of angle $\Delta\theta_t = {(\Delta s_R - \Delta s_L)}/{m}$ in each unit time, as measured by the external sensors in the case of known current position conditions of the robot, where Δs_L and Δs_R represent the displacements of the left and right wheels, respectively. Therefore, if the location of the robot is $p_t(X_t, Y_t, \theta_t)$, the estimated position point of the next time should be $p_{t+1}(X_{t+1}, Y_{t+1}, \theta_{t+1})$, where $u_t = (\Delta d_t, \Delta\theta_t)^{\mathrm{T}}$ is defined as the input of the odometer model in each time interval. Thus, the motion model of robot can be defined as [**19**][**4**].

$$Z(p_t, u_{t-1}) = \begin{bmatrix} x_t \\ y_t \\ \theta_t \end{bmatrix} + \begin{bmatrix} \Delta d_t \cos(\phi_t + \Delta\theta_t/2) \\ \Delta d_t \sin(\phi_t + \Delta\theta_t/2) \\ \Delta\theta_t \end{bmatrix} \tag{5}$$

Equation (5) can be rewritten into:

$$Z(p_t, u_{t-1}) = \begin{bmatrix} x_t \\ y_t \\ \theta_t \end{bmatrix} + \begin{bmatrix} \frac{(\Delta s_L + \Delta s_R)}{2} \cos(\phi_t + \frac{\Delta s_L - \Delta s_R}{2m}) \\ \frac{(\Delta s_L + \Delta s_R)}{2} \sin(\phi_t + \frac{\Delta s_L - \Delta s_R}{2m}) \\ \frac{\Delta s_L - \Delta s_R}{2m} \end{bmatrix} \tag{6}$$

The realization of dead reckoning for the proposed mowing robots is to use the electric compass to obtain the current heading angle of robot and utilize the encoders installed inside both wheels to compute and estimate the rotation angles of both wheels and displacement. Combined with the absolute positioning information, as obtained by the electric compass, it can adjust its heading orientation. If θ_T represents the expected orientation angle, the angle between the robot and magnetic north is $\theta = \tan^{-1}(\mathrm{Y}/\mathrm{X})$; therefore, the heading angle of the robot should be adjusted by:

$$\varepsilon = \theta_T - \theta \tag{7}$$

By iteration of (7), the heading angle can be obtained. After the introduction of the PID controllers, the outputs of V_L and V_R can be determined to adjust the robot to return to the expected heading.

3. MOTION SPEED RECKONING

In the process of robot movement, the encoders of both wheels can obtain the travel distance information of both wheels. The differentiation of the distance against the time can result in the motor rotation speeds of both wheels, as shown in (8) and (9):

$$\hat{V}_L = \frac{\Delta s_L}{\Delta t} \tag{8}$$

$$\hat{V}_R = \frac{\Delta s_R}{\Delta t} \tag{9}$$

where Δt is the sampling time. When the electric compass and PD controller can adjust the robot to the targeted heading, how to maintain the robot to move in a linear path depends on the encoders. Provided the settings of the outputs of the encoders of both wheels are known, the robot movement can maintain a straight line. In addition, the encoders can obtain information regarding the rotation angle, through which the rotation speed information can be indirectly obtained. The PI controller enables the rotation speeds of both wheels to maintain the same speed, thus, without skidding or a bumpy road surface, the path of the robot can be straight.

4. PID CONTROLLER

The PID controller is an indispensable element commonly seen in the feedback control system, which compares the output of the feedback system, and the expected reference value and error are then regarded as the input of the PID controller. The new input value can allow the feedback system output to reach or

maintain the expected value. The PID controller is able to adjust the system input according to the output values of the feedback system, which renders the system more stable. In the PID control system, the errors can be eliminated by three computational methods, and future errors can be predicted according to the average of previous errors and changes in the errors, as shown in (10).

$$U(t) = K_P e(t) + K_I \int_0^t e(t)dt + K_D \frac{d}{dt} e(t) \tag{10}$$

where $U(t)$ is the control amount, $e(t)$ is the error value, K_D is the differential coefficient, K_P is the proportional coefficient, and K_I is the integral coefficient. In the proposed system, the encoders, electric compass, and PID controller are somewhat correlated. This study used two sets of PID controllers to control the rotation speeds of both wheels. First, through (8) and (9), the distance values, as measured by the encoders of both wheels, are converted into the rotation speeds of both wheels. The moving speeds of both wheels and expected speeds, that is, V_T^L and V_T^R have errors of E_L and E_R, as shown in (11) and (12).

$$E_L = V_T^L - \hat{V}_L \tag{11}$$

$$E_R = V_T^R - \hat{V}_R \tag{12}$$

Through the adjustment of three parameters, including K_P, K_I, and K_D, the rotation speeds of both wheels can be maintained as the expected values. In general, the three control parameters of the PID control system are not used at the same time. In this paper, when the motor rotation speed error amount is zero, the control system requires output values to use PI controller. When the motor error amount is zero, the control system uses the PD without requiring the output (the latter is used for angular control), while K_P allows the system output response to rapidly approach the target value. However, an excessive response may generate overshoot and even instability. Where K_D adjusts the system response time and can suppress overshoot; while K_I can reduce the steady state error.

This study uses the trial-and-error method combined with the Ziegler-Nichols method to regulate the PID parameters. First, the K_P is adjusted until the system generates a shock and the system response reaches the boundary steady state. The proportional gain reaching the condition is defined as K_P^C. Next, suitable K_I and K_D parameters are determined. Table 1 illustrates the parameters used by the PID controller, where, the period of time is defined as T_c.

If a PID controller and encoders are used, various factors, such as skidding, a rough road surface, and the error of tire diameters, may lead the robot to deviate from the expected route. In this case, an electric compass should be applied to adjust the heading angle. When the robot is off track, angle of magnetic north and expected orientation angle have errors in the heading angles. The error can be input into the PID controller to adjust the angle by PD control before switching back to the PI controller.

In addition to the use of PID control, many other control methods can be used, such as sliding fuzzy control, neural network control, adaptive control, etc. However, in the actual study, when it is difficult for the controlled system to obtain an accurate mathematical model, the control theories will be more difficult to achieve and apply. In this case, the controller structure and parameters should be adjusted according to experience and occasions of use. The application of the PID control technology is convenient and effective in the adjustment of parameters. This is one of the reasons such technology is widely preferred by the industry.

SYSTEM DESCRIPTION

This section explains the mechanism design process, including the planning of a prototype of robot, and the design of the mowing disc and motor drive coupling; in addition, it includes software and hardware planning and design, and integration of the entire system.

1. Mechanism Design

The proposed mower's mechanism includes the load platform, the transmission mechanism, and mowing device **[20]**. The mechanism design is as shown in Fig. 1. The total weight is 30 Kg. Regarding the load platform design, first, a 60500.5 (lengthwidththickness) cm aluminum board is served as loading/carrying platform, on which circuit boards, sensor module, and fuel cell are applied. The four points at the corners of the board are connected with the aluminum frame, on which the acrylic board is placed, which consists of front and rear pieces. The skidding rails are installed between the front piece of the acrylic board and the frame to allow the acrylic board to move forward and backward. Therefore, it is convenient for the user to check the circuits below the acrylic board. The rear board of the acrylic board is fixed in the aluminum strips and the laptop is placed above it. The frame is sealed by using the acrylic board to protect the internal circuit system and sensors. Below the loading platform, two DC motors of 25-kg torque and a mowing motor are installed.

Regarding the transmission mechanism design, the mowing robot has four wheels, and is driven by the dual front-wheels, while the two rear wheels are the auxiliary wheels. The front wheel diameter is 30 cm, and its width is 8 cm. The diameter of rear two wheels is 20 cm, and its width is 6 cm. The coupling mechanism between the motor and the wheels includes an L-shaped aluminum board to affix the motor, the internal coupler, and the two bearing seats. The L-shaped aluminum is mainly used to elevate and affix the motor in order that it can be smoothly linked with the wheel rims. The internal long coupler is to connect the motor and the wheel rims, and the two bearing seats are to support the coupler to enhance the stability of the motor during operation. The completed structure is as shown in Fig. 2.

The design of the mowing device mainly includes a high rotation speed motor and mowing disc. The mowing motor torque is 1.2 Kg, rotation speed is 3750 rotor per minute (rpm), and the mowing disc is round and affixed in one of the three holes of the extended motor axis. The adjustable height method provides the user to easily change the mowing height. The mowing tool has been changed from the original bowstrings to a jagged blade to effectively mow weeds and free the user from replacing the bowstrings. Figure 3 demonstrates the appearance of mowing mechanism.

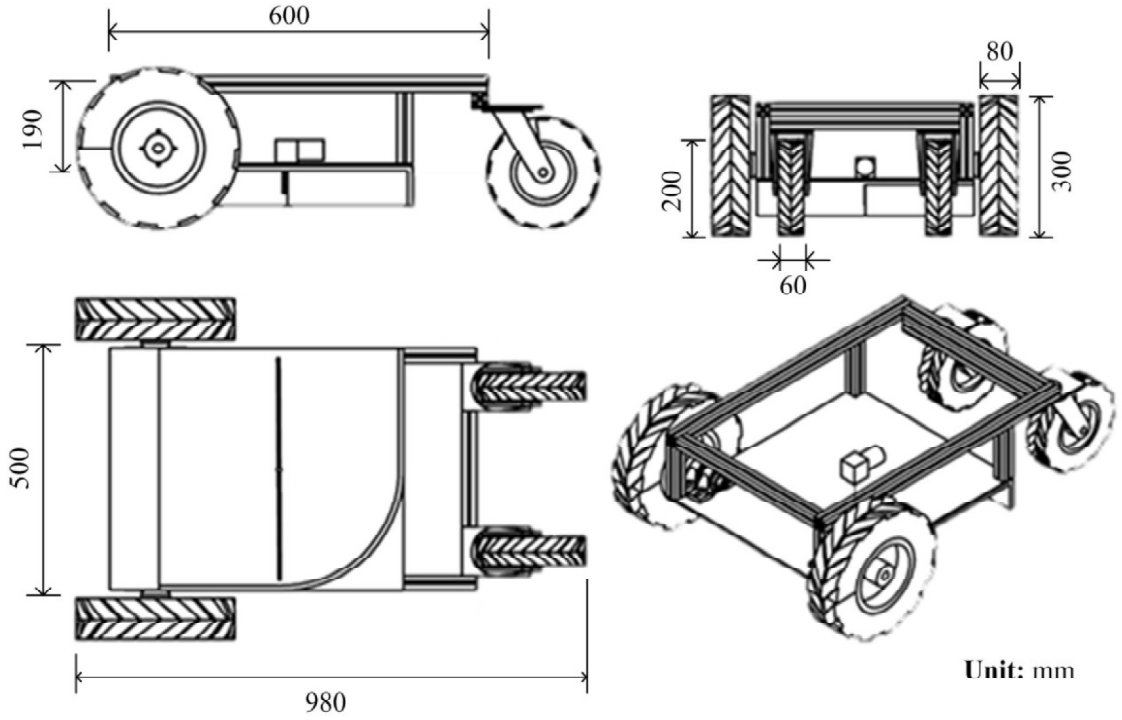

Figure 1: Mowing robot mechanism prototype

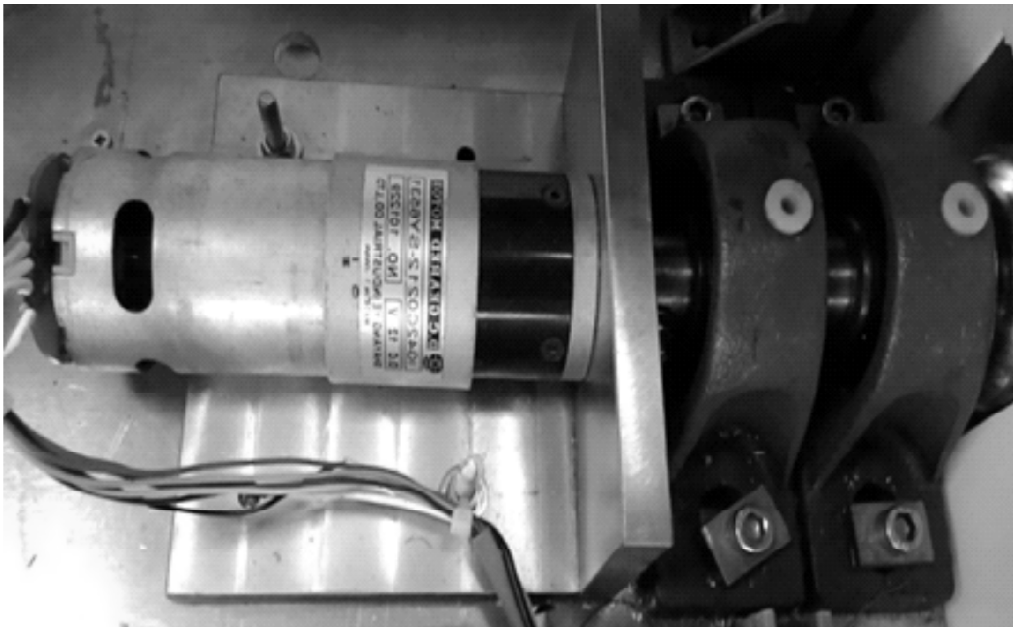

Figure 2: Motor seat and coupler

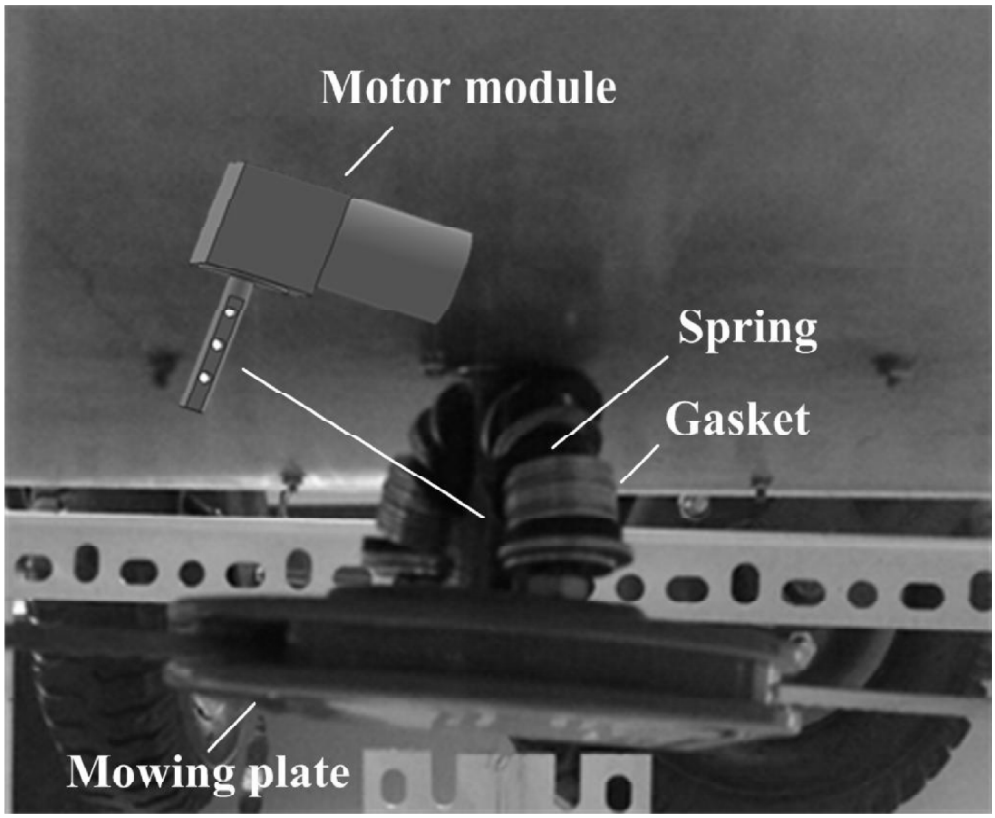

Figure 3: Mowing device (motor module and jagged blade mowing plate)

2. Hardware Architecture

The mowing robot hardware architecture consists of a sensing module, heading control module, motor driving module, mowing module, and alarm module. The system architecture is as shown in Fig. 4. The sensing module mainly contains ultrasonic sensors, electric compass, and laser scanner. There are 6 sets of ultrasonic sensors installed in the front part of the robot (2 sets) and both sides of the robot (two sets on

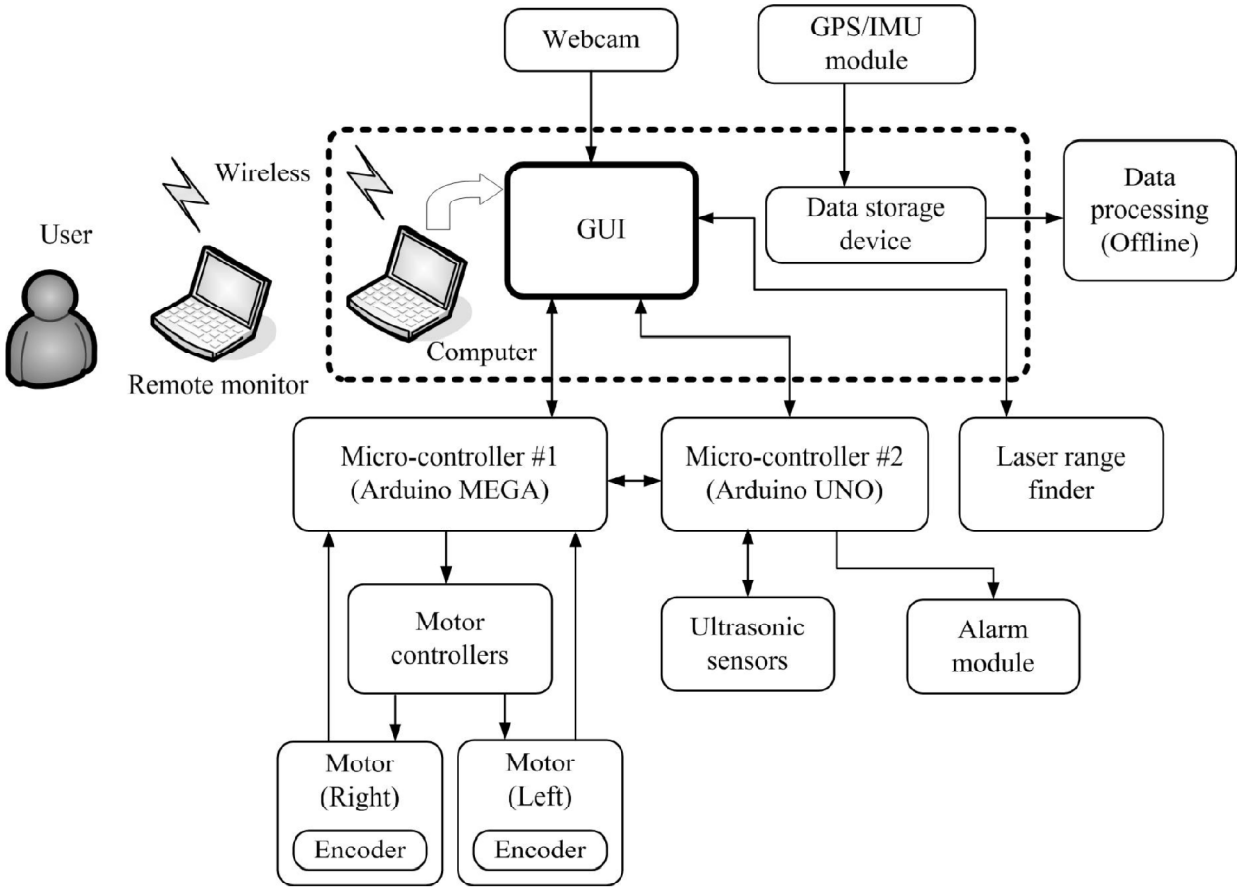

(a)

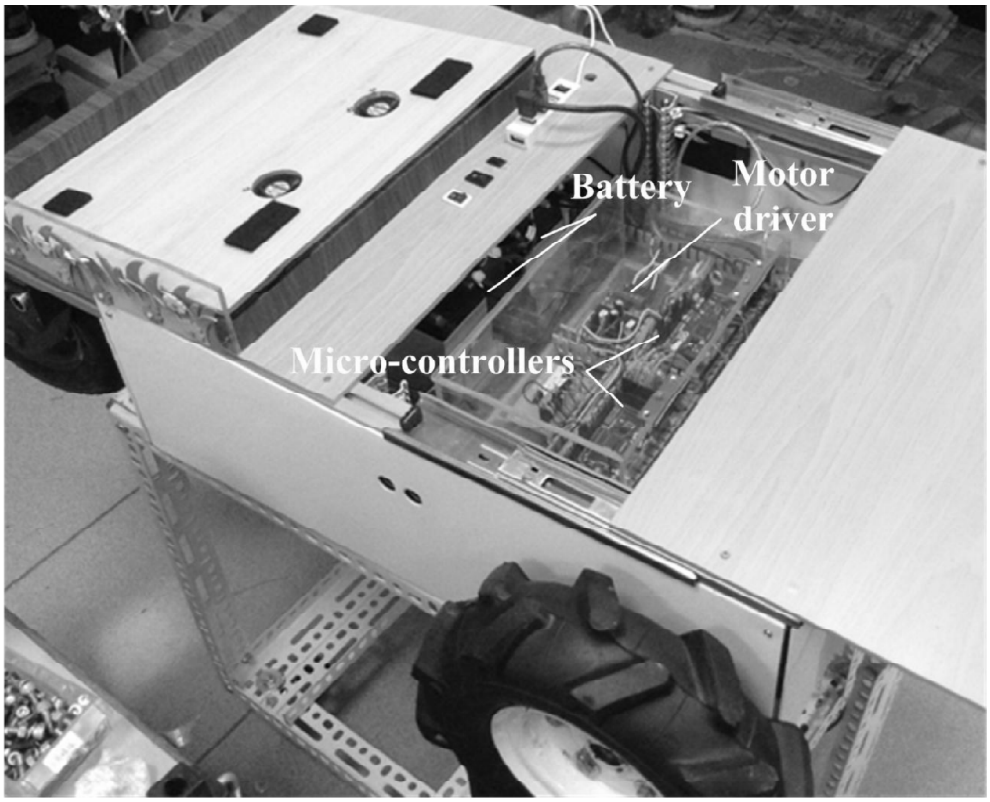

(b)

Figure 4: Mowing robot system architecture. (a) System diagram; (b) The appearance of control box

each side). Its main function is to detect whether there are any approaching objects in the surroundings of the mowing robot, which is combined with an alarm system. The electric compass device can obtain the current heading data of the robot and provide the data to the navigation control module for heading correction. The laser scanner can provide the robot with the orientation of the area without mowing. The data can be directly transmitted to the computer through the universal serial bus (USB) interface and displayed on the graphical user interface (GUI); the navigation control module consists of computer and two sets of Arduino microcontrollers. Wherein, the Arduino UNO controller is used to receive the data from the six sets of the ultrasonic module, and the Arduino MEGA controller is to receive the orientation data sent back by the electric compass and pulse signals sent back by the encoders of the two sets of motors. Combined with the internal PID software program, it drives the dual motors and the DC motor inside the mowing module. The alarm module includes a buzzer and warning lights. The module can prevent people from entering the warning area by the warning sound to improve safety in use. In addition, the robotics mower is equipped with GPS/inertial measurement unit (IMU) navigator which to achieve the function of positioning data recording.

3. Software Interface

The proposed system plans a GUI implemented by the Labview software. The software provides simple graphic connection blocks for users to design a suitable GUI. In the design process, the user is not required to input any instruction command, but guides the object to the interface framework and connects it with the corresponding object before setting the parameters. Figure 5 illustrates the appearance of the proposed GUI. The interface can be mainly divided into communication transmission settings, control mode, and monitoring window. Regarding the communication transmission settings, the interface provides the user with functions to set the number of communication port, and the maximum and minimum detection distances of laser rang finder [**21**]. The ranges within the orientations of 240° in front of the robot will be displayed on the interface. It scans and measures a group of range values every 27 degrees. In total, nine range values of mowing detection area can be displayed. The laser range finder is connected via USB with the computer. Then, the NI-VISA communication firmware is installed to facilitate the connection and transmission of data between the computer and the laser range finder. The data measured by the laser range finder mainly allows the user to judge the mowing orientations in front of the robot by manual mode. Regarding the control mode, the interface provides automatic and manual control modes. In the automatic mode, the robot can move along a set path. Through the dead reckoner and PID controller, it can complete linear moving, cornering, and obstacle avoidance. When the user switches to the manual control mode, the user can take advantage of the four buttons to control the robot in moving forward, turning left, turning right, and moving slowly forward. The graphically controlled buttons use the “Radio Buttons” object for the command transmission between the Arduino controller and GUI. The object is provided by the toolkit of Arduino (Arduino package). The user must only install the JKI VI Package Manager (VIPM) to add the components of the Arduino package to the Labview library. Finally, regarding the monitoring window, the real time webcam on the interface can provide the user with easy remote monitoring. For example, when the robot encounters an emergency in movement, the user may immediately manually control the robot to prevent loss of control in the remote end. The remote connection is realized by the remote connection of two computers through the Team viewer software. When the connection is complete, the user may directly observe the image of the area in front of the robot on the remote computer screen to realize the purpose of monitoring.

4. Navigation and obstacle avoidance

Figure 6 demonstrates the system control flowchart. First, the desired mowing path data is burned into the memory on micro-controller board. Next, the graphical user interface (GUI) is evaluated through Labview software. The user can select either automatic mode or manual mode to control the mowing robot. The robot can follow the desired path which the user pre-defined under the automatic mode. When the robot

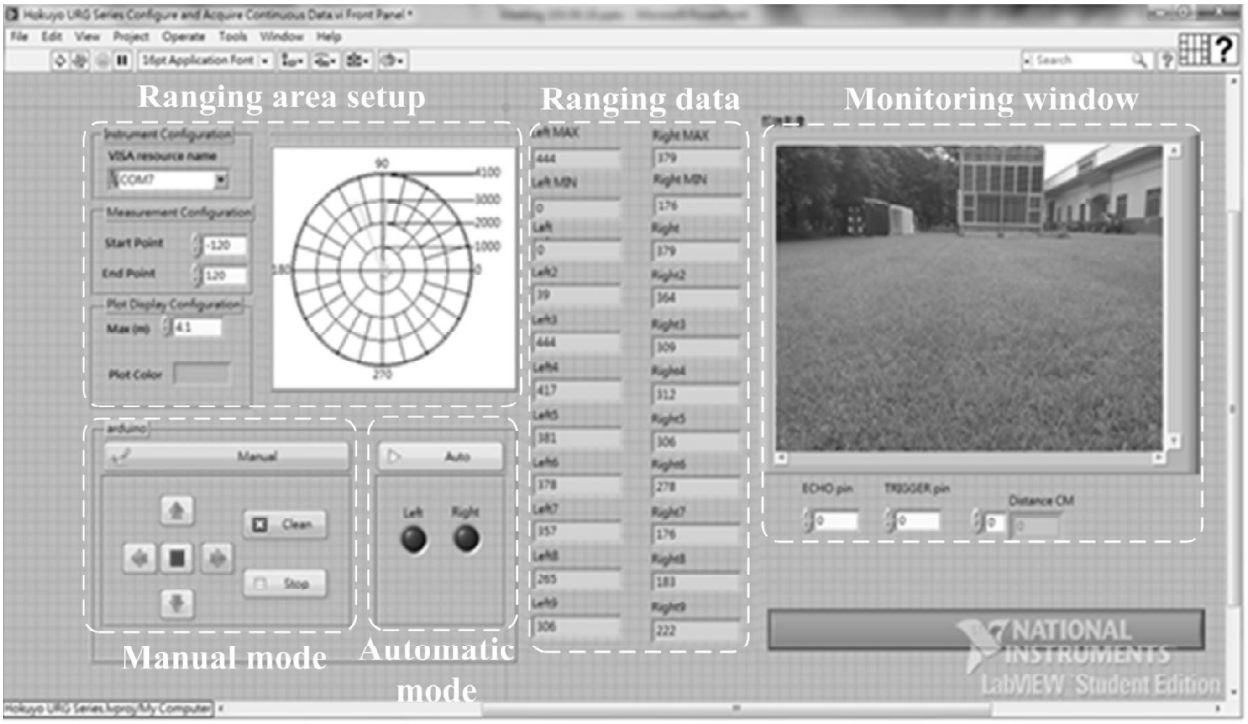

Figure 5: Labview-based graphical user interface

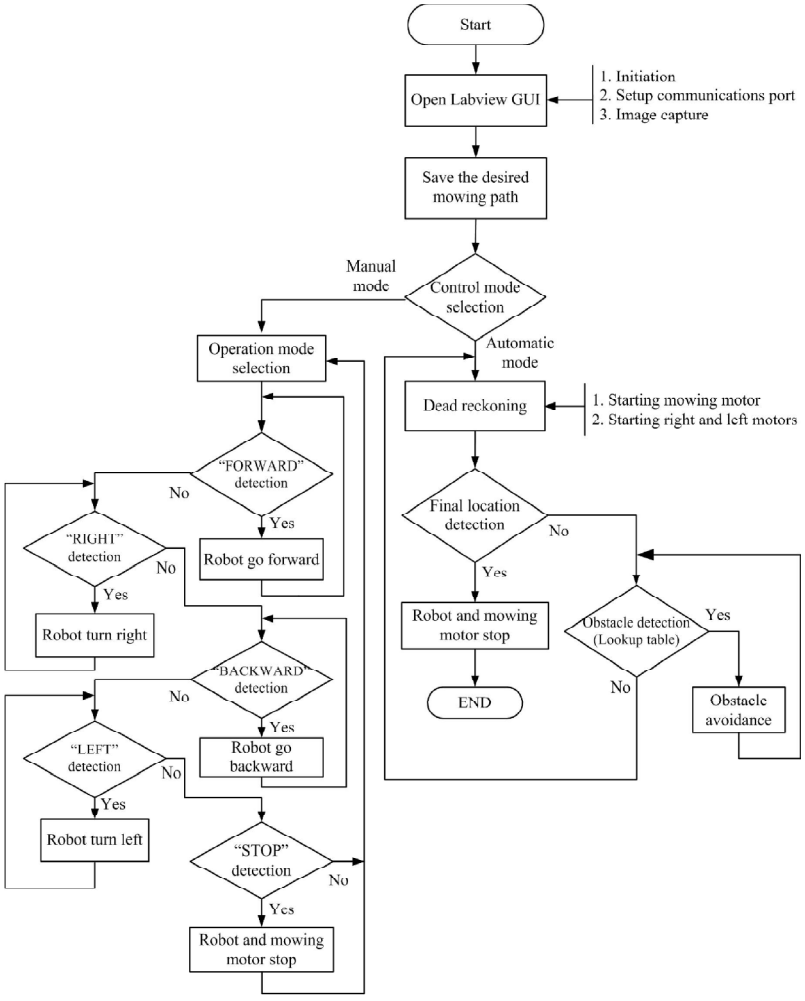

Figure 6: The flowchart of robot operation

detects an obstacle in the surrounding area, the system will switch from the navigation mode to the obstacle avoidance mode. After confirmation of avoidance, it will switch back to the navigation mode. The head of the mowing robot and both sides of the robot are installed with ultrasonic sensors. The distances between the two sets of ultrasonic sensors are 40 cm. As the ultrasonic detection angle is 15 degrees, the effective detection range is 100 cm. The configuration and implementation of the ultrasonic module are as shown in Fig. 7. The detection range is divided into A, B, C, D, E, and F area. When the feedbacks of the six sets of ultrasonic modules are transmitted to the Arduino controller, the internal program of controller will carry out the object detection function. The function of obstacle avoidance mainly depends on the logic computational table (as shown in Table 2) parameters for obstacle avoidance. The detection results of the six ultrasonic sensors can be used to determine the rotations of the motors to allow the robot to move forward, turn left, and turn right, thus, realizing the function of obstacle avoidance.

RESULTS AND DISCUSSION

This section discusses the performance test results of the proposed mowing robot, including three kinds of experimental results, that is, the linear moving experiment, static and dynamic object obstacle avoidance experiment, cattle plow, and spiral plow mowing experiment. Each experiment was repeated ten times. Prior to various experiments, the sensors are corrected, battery power is confirmed, and the preset path data of the robot is stored inside the controller. The experimental site is located in 120.6062 degrees east longitude and 22.64658 degrees north latitude.

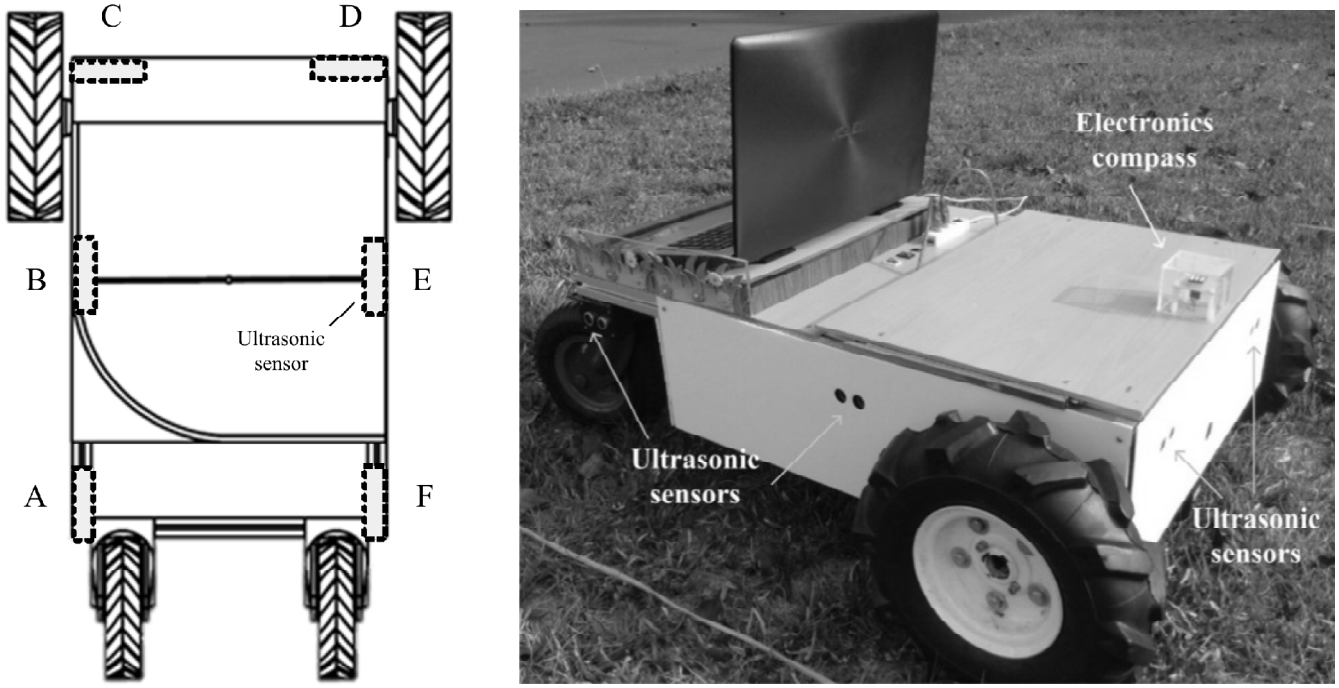

Figure 7: Sensing module. (a) Ultrasonic module configuration; (b) Robot implementation

Table 1
PID parameters of the Ziegler-Nichols method

Type	*KP*	*KI*	*KD*
P	$0.5 \times K_P^C$	-	-
PI	$0.45 \times K_P^C$	$(0.54)/T_c$	-
PID	$0.6 \times K_P^C$	$1.2 \times K_P^C$	$0.0075 \times K_P^C \times T_c$

Table 2
Ultrasonic obstacle avoidance logic decisions

Logic state			*Output PWM*			
A & B	*C & D*	*E & F*	*Left motor*	*Right motor*	*Robot Behavior*	*Alarm Status*
1	1	1	0	0	Stop	ON
1	1	0	200	100	Turn right	OFF
1	0	Í	220	220	Forward	OFF
0	1	1	100	200	Turn left	OFF
0	1	0	200	100	Turn right	OFF
0	0	1	220	220	Forward	OFF
0	0	0	240	240	Forward	OFF

Note: "1" represents the existence of an obstacle; "0" represents there is no obstacle ; "Í" depict "1" or "0"; "&" represents "AND" logic operator.

1. Linear moving

The experiment tested the straight movement of the robot. The distance was 10 m. The robot completed dead reckoning through the encoders, and used the PID controller to adjust the rotation speed of speed. The PID controller can regulate the right and left output voltage of motor drivers which results in different speed of motors. It is noteworthy that PI control method is only utilized to maintain the same velocity between right and left motor. The parameters of PID controller for right motor are $K_I = 0.6$, $K_P = 0.08$, and $K_D = 0$; The parameters of PID controller for left motor are $K_I = 0.6$, $K_P = 0.0765$, $K_D = 0$.

Figure 8(a) shows the robot moving distance, while Fig. 8(b) illustrates the movement path. As seen, ranging error was within 3.5 cm. For ten realizations, statistics computed are 3.2 ± 0.1 (standard deviation [SD]) cm in ranging error.

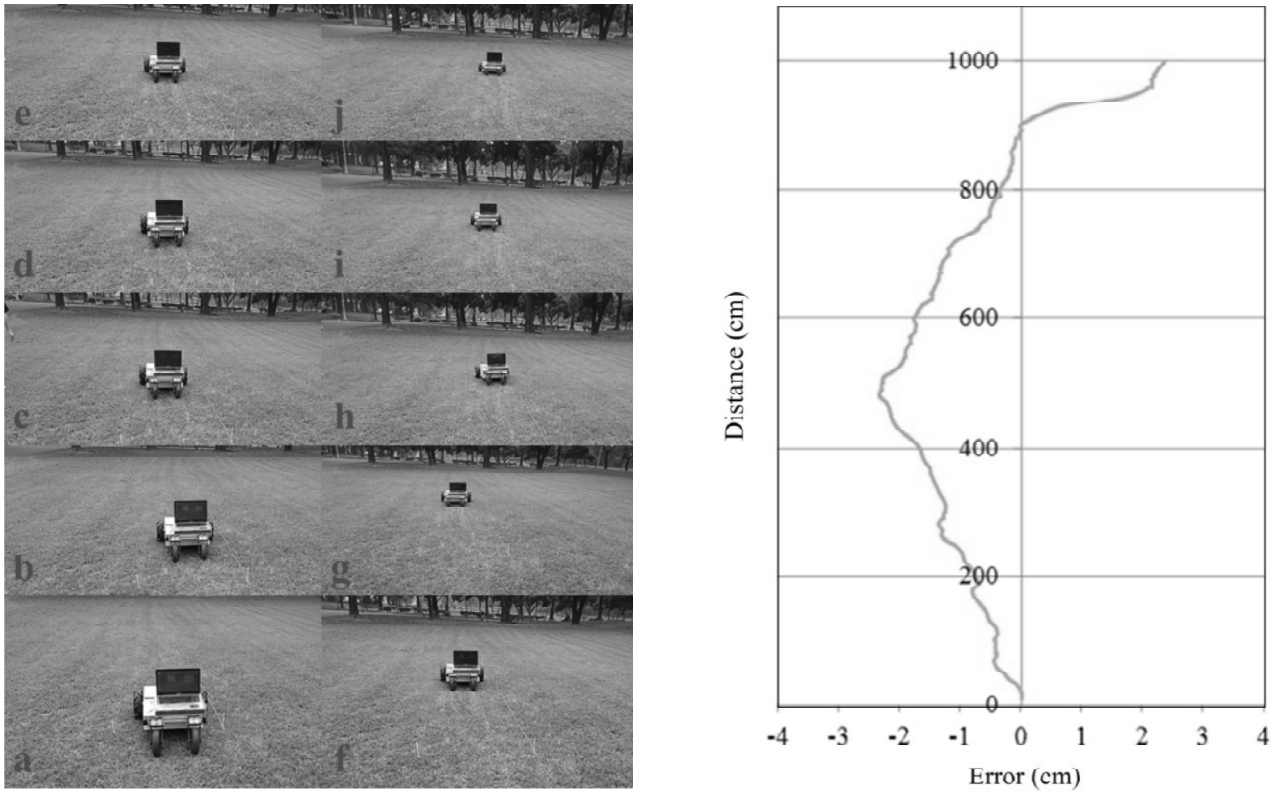

Figure 8: Robot linear moving experiment. (a) Moving process; (b) Linear moving error

2. Obstacle avoidance

The obstacle avoidance experiment was to observe the obstacle avoidance effect by placement of an obstacle. The experiment was further divided into fixed object obstacle avoidance testing and human movement obstacle avoidance testing. Figure 9(a) shows the movement path of the robot in the fixed object obstacle avoidance experiment. As seen, the robot can complete fixed obstacle avoidance. The human movement obstacle avoidance was to test whether the robot can automatically avoid any person appearing suddenly in front of the robot. The robot movement path is as shown in Fig. 9(b). The movement coordinates data of the robot were provided by the MTI-G device, and described by Google Map.

3. Cattle plow and spiral plow mowing

The cattle plow and spiral plow mowing experimental areas were square areas of 3.5 meters in length and width. The experiment tested the robot's mowing efficiency and analyzes the coverage rate after the first mowing. The coverage rate of α is defined, as shown in (13).

$$\alpha = \left(1 - \frac{\gamma}{\beta}\right) \times 100\% \tag{13}$$

β and γ denote mowing area and the area without mowing. Figure 10 illustrates the path planning of the cattle plow and spiral plow mowing experiments. In cattle plow mowing, the system stored the path data. When the robot moved, encoders and the PID controller were used to compute the movement distance and

(a)

(b)

Figure 9: Obstacle avoidance experiment (a) moving path (fixed obstacle); (b) moving path (moving obstacle)

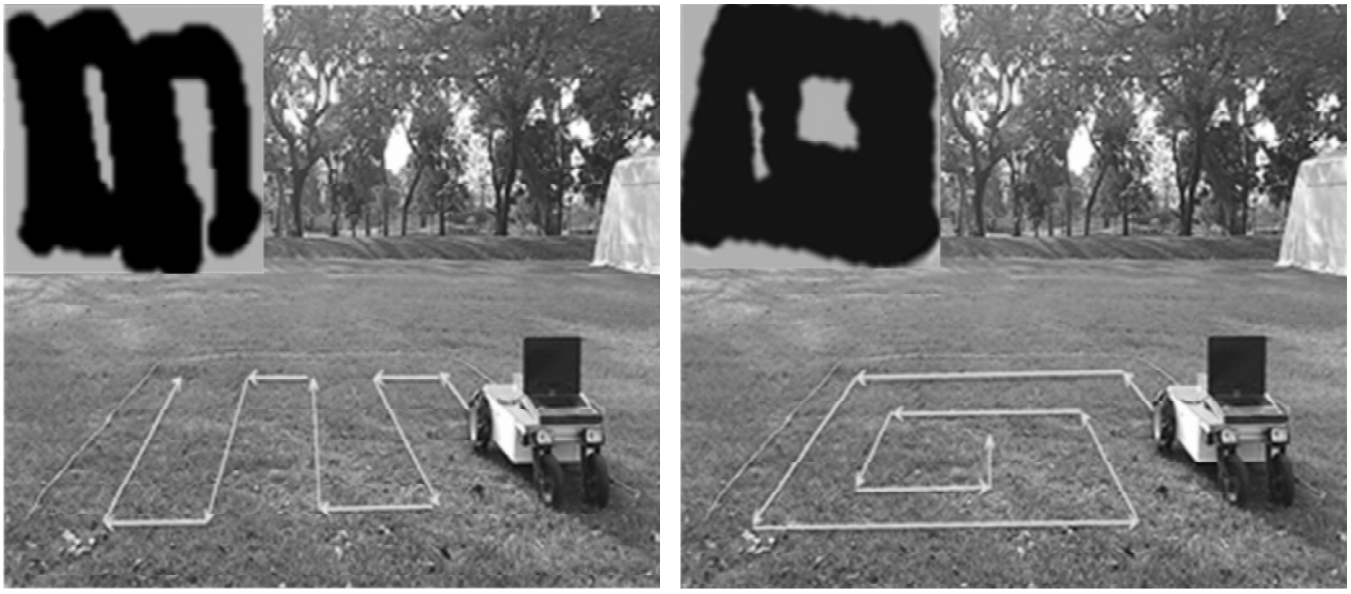

(a) **(b)**

Figure 10: Mowing path planning and mowing experimental path (without sensor calibration). (a) Cattle plow; (b) Spiral plow

keep the robot moving in a straight line. Finally, the angular values sent back by the electric compass were used to determine whether the robot has achieved the expected rotation angle of 90 degrees. The above actions, repeated five times, completed the cattle plow movement. The PID parameters are the same as linear moving test. The mowing area shown in Fig. 10 is black line denoted mowed area. The coverage rate are 67% and 72.8% for cattle plow and spiral mowing, respectively. Meanwhile, the ranging error of cattle plow and spiral mowing are 3.4±0.2 cm and 3.1±0.1 cm, respectively. As the angular data received by the robot during turning are not accurate, it can result in turning errors and reduced coverage rate. Therefore, the calibration of electronic compass is required repeatedly. In addition, the modified cattle plow method is proposed to increase the mowing coverage rate which is shown in Fig. 11. The path data of modified cattle plow is stored in the control system, which performs the robot movement operation from path #1 to path #3.

Table 3 illustrates the average coverage rate under different sizes of mowing area (with sensor calibration). Each of experiment tests under different sizes of mowing area is performed by ten times. The mowing results demonstrate that higher average coverage rate is obtained by using modified cattle mowing method in contrast to the use of others. However, the use of modified takes longer mowing time and results in higher power consumption.

Table 3
Coverage rate comparison under different mowing method (with sensor calibration)

Mowing area (Length (L) × Width (W) (m))	*Average coverage rate (three realizations)*		
	Cattle plow	*Modified cattle plow*	*Spiral*
3.5×3.5	80 %	90 %	82 %
4×4	79 %	88 %	82 %
4.5×4.5	77 %	87 %	83 %
5×5	74 %	84 %	83 %
5.5×5.5	75 %	85 %	84 %

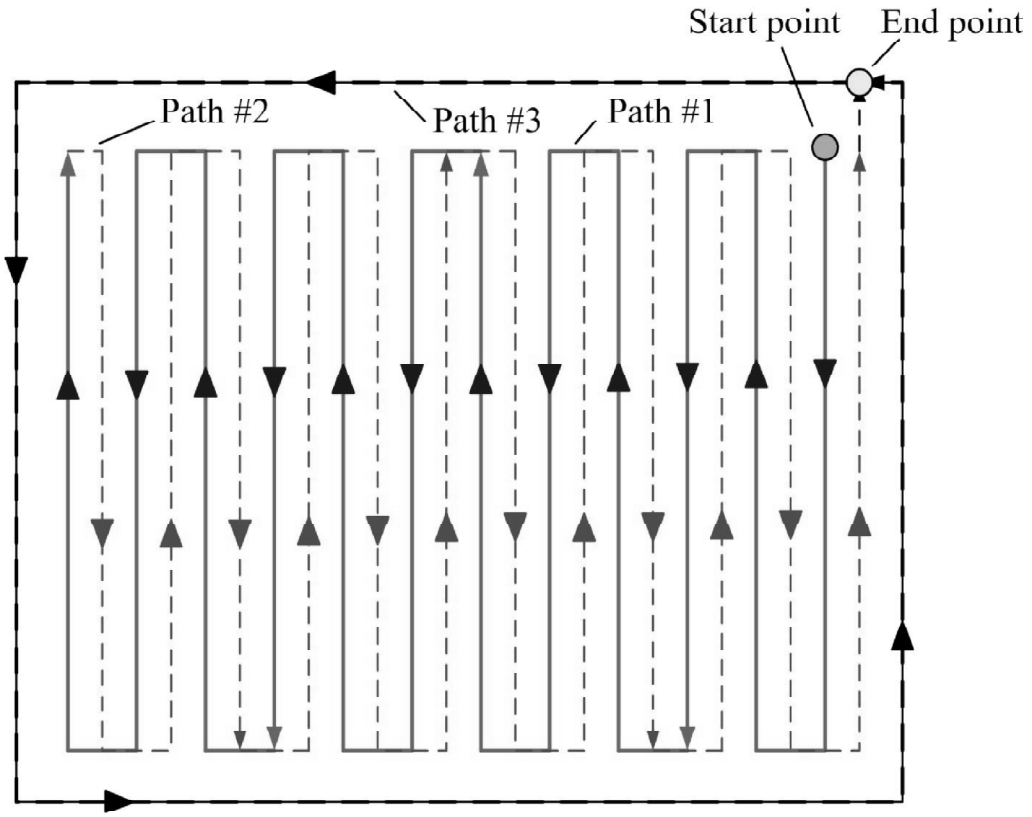

Figure 11: Modified cattle plow path planning

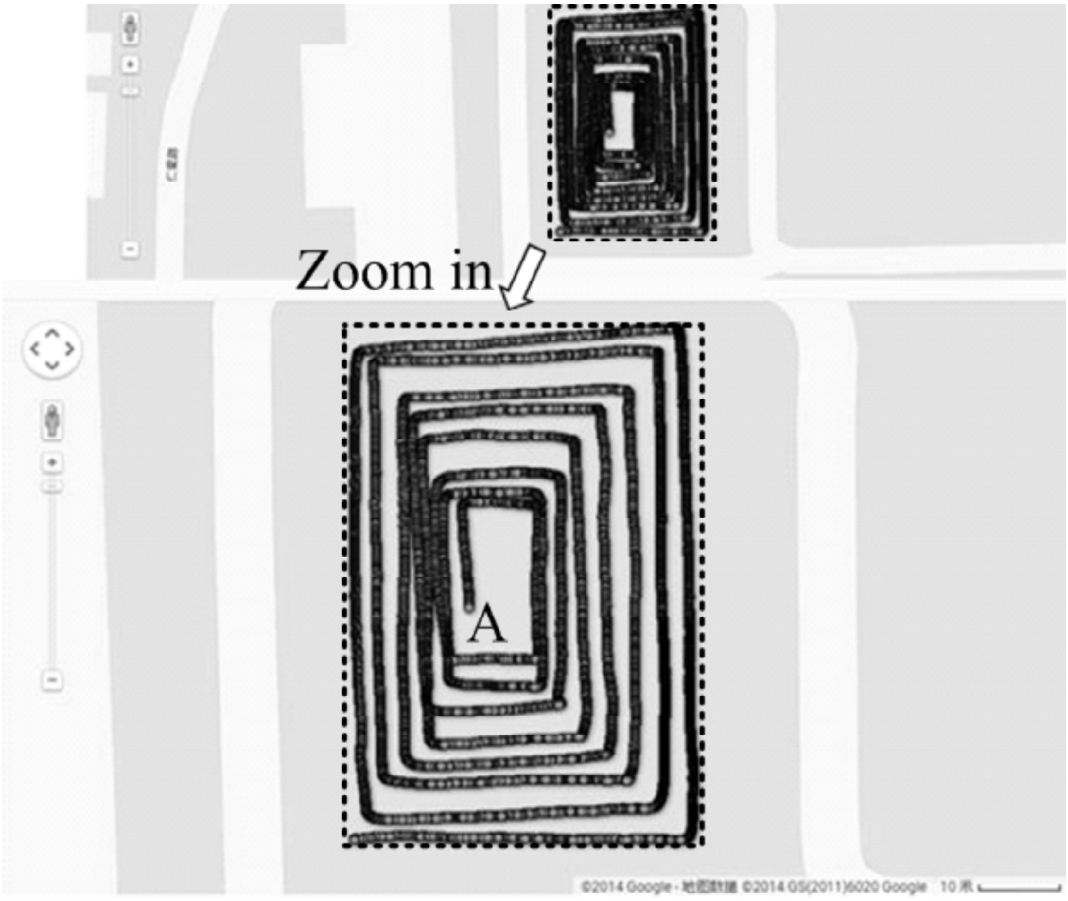

Figure 12: The mowing experimental path with wide area

Finally, the robot endurance test is performed in the real field. Fig. 12 demonstrates the maximum area of mowing which the robot mows. It is totally 1400 m^2 in area and the coverage rate of mowing is 84.3 %. However, the robot stops moving at "A" point which is according to battery capacity, which results in un-mowed areas located in middle area. Nevertheless, the proposed robotic mower is sufficient to provide the user to manage the home lawn smoothly.

CONCLUSION

This study proposed an electric mowing robot prototype, which integrates the remote control interface and micro controller. Free from the disadvantages of waste exhausts and high noise of conventional mowers, the proposed robot can automatically mow along a preset path. The proposed robot has the following functions: 1) in the case of a load of 35 kilograms, the speed can be up to 6 cm /second, and average endurance can be 1030 m; 2) the linear movement ranging error is 3.2±0.1 (standard deviation [SD]) cm; 3) 6 sets of low-cost ultrasonic sensors can realize 270-degrees of obstacle avoidance; 4) mowing average coverage rate is between 74 % and 90 % (depend on mowing path); 5) has remote monitoring capability. In the future, IMU sensors and attitude calibration platforms may be added to allow the robot to move on bumpy surfaces. Meanwhile, an automatic charging device can be added to increase flexibility in the use of the robot. This robot can be applied in the maintenance and cleaning of a variety of turfs, as well as the cleaning and management of waste cultivated agricultural land or fallow land.

Acknowledgment

Many thanks are due to anonymous reviewers for their time and valuable comments. This work has been supported by the Ministry of Science and Technology, Taiwan, Republic of China, under grant no. MOST 103-2221-E-020-041.

Conflicts of Interest

The authors declare no conflict of interest.

Author Contributions

The overall scheme, robot platform is designed by Yang Chen; he also wrote the program, performed and analyzed the experimental data. Chung-Liang Chang wrote the paper and advised the work at all stages. The final manuscript has been read and approved by both authors.

References

[1] iRobot Co., Roomba, data available: http://www.irobot.com/For-the-Home/Vacuum-Cleaning/Roomba.aspx (Retrieved 12 January 2015).

[2] Sandia National Laboratories, Gemini-Scout, data available: http://www.sandia.gov/research/robotics/_assets/documents/Gemini_Scout_Handout_Final.pdf (Retrieved 10 January 2015)

[3] C. L. Chang, J. F. Chen, J. H. Jhu, "Design and implementation of a gardening mobile robot with embedded face-tracking system," IEEE International Symposium on Intelligent Signal Processing and Communication Systems (ISPACS 2012), Tamsui, New Taipei City, Taiwan, pp. 239–244, 2012.

[4] C. L. Chang and J. H. Jhu, "Zigbee-assisted mobile robot gardener," 2013 CACS International Automatic Control Conference, Nantou, Taiwan, pp. 41–46, 2013.

[5] M. Norremark, H. W. Griepentrog, J. Nielsen, H. T. Sogaard, "The development and assessment of the accuracy of an autonomous GPS-based system for intra-row mechanical weed control in row crops," *Biosystems Engineering*, Vol. 101, pp. 396–410, 2008.

[6] D. C. Slaughter, D. K. Giles, D. Downey, "Autonomous robotic weed control systems: A review," *Comput. Electron. Agric.*, Vol. 61, pp. 63–78, 2008.

[7] G. Freitas, J. Zhang, B. Hamner, M. Bergerman, G. Kantor, "A low-cost, practical localization system for agricultural vehicles," Intelligent Robotics and Applications: *Lecture Notes in Computer Science*, Vol. 7508, pp. 365–375, 2012.

[8] C. L. Chang, B. H. Wu, and Y. C. Huang, "Outdoor mobile field robot navigation, *Coordinates*, Vol. 9, pp. 10–19, 2013.

[9] C. L. Chang, B. H. Wu, and C. C. Chang, "Autonomous field robotic vehicle with embedded multi-sensor system for agricultural applications," *ION International Technical Meeting* (ITM), pp. 1077-1084, San Diego, California, USA, January 24–26, 2011.

[10] The Old Lawnmower Club. Mower History. The Old Lawnmower Club. Data available from: http://www.oldlawnmowerclub.co.uk/aboutmowers/history. (Retrieved 23 November 2014).

[11] N. Nourani-Vatani, M. Bosse, J. Robert, M. Dunbabin, "Practical path planning and obstacle avoidance for autonomous mowing," Australasian Conference of Robotics and Automation (ACRA), Auckland, New Zealand, pp. 1–9, 2006.

[12] M. Wasif, "Design and implementation of autonomous Lawn-Mower Robot controller," IEEE 7th International Conference on Emerging Technologies (ICET), Islamabad, Pakistan, pp. 1–5, 2011.

[13] A. D. Smith, H. J. Chang, and E. J. Blanchard, "An outdoor high-accuracy local positioning system for an autonomous robotic golf greens mower," IEEE International Conference on Robotics and Automation (ICRA), Saint Paul, MN, USA, pp. 2633–2639, 2012.

[14] J. Yang, S. J. Chung, S. Hutchinson, D. Johnson, "Vision-based localization and mapping for an autonomous mower," 2013 IEEE/RSJ International Conference on Intelligent Robots and Systems (IROS), Tokyo, Japan, pp. 3655-3662, 2013.

[15] Robomow Co., Mowers, data available: http://robomow.com/en-GB/product-category/mowers/ (Retrieved 16 January, 2015).

[16] Husqvarna AB (publ), Automower, data available: http://www.husqvarna.com/us/products/robotic-mowers/husqvarna-robotic-mowers-for-homeowners/ (data access date: 16 January, 2015).

[17] Deere & Company. Tango E5. Data available from: https://www.deere.com/en_INT/products/equipment/autonomous_mower/tango_e5/tango_e5.page#viewTabs (Retrieved 3 January 2015)

[18] Mow-By-Sat project. Data available from: http://mow-by-sat.diees.unict.it/ (data access date: 16 January, 2015).

[19] P. Jensfelt, H. I. Christensen, "Pose tracking using laser scanning and minimalistic environmental models," IEEE Trans Robot. Automat., Vol. 17, 138–147, 2001.

[20] C. Yang and C. L. Chang, "Design and implementation of an autonomous robotic lawn-mower," 2nd International Conference of Multi-Disciplines of Engineering on Advanced Technology and Environmentalism Design (MDEATED 2014), Tainan City, Taiwan, pp. 209-210, 2014.

[21] HOKUYO AUTOMATIC Co., Ltd. URG-04LX-UG01. 2009. Data available from: https://www.hokuyo-aut.jp/02sensor/07scanner/urg_04lx_ug01.html (Retrieved 13 May 2014).